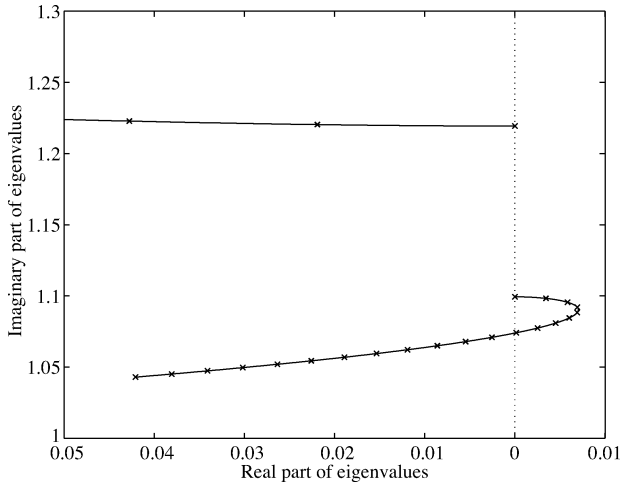


**Fig. 6 Effect of proportional damping on the stability characteristics of the airfoil.**

the $p$ and $k$ solutions. For this case the system is neutrally stable (as predicted by the $p$ method and ambiguously by the $k$ method). Now stiffness-proportional viscous damping is added, and the system is solved using the $p$ method. Figure 6 shows the change in the eigenvalues of the system with $c$ (damping proportionality factor) ranging from $c = 0$ to 0.2, with 0.01 increments in $c$ denoted by the cross marks. Here it is clear that even for positive structural damping one of the roots becomes unstable for a while and then becomes stable. Hence, there exists a value of $g$, which, if added, causes the system to return to neutral stability. The $k$ method does predict correctly this second value of $c$ (apart from $c = 0$) for which the system is neutrally stable. This insight provided by the $k$ method is important because in realistic problems there is a distinct possibility of small structural damping where the $k$ method accurately predicts the possibility of instability.

The reason for small stiffness-proportional damping to lead to destabilization of the system might be surprising at first, but such a destabilizing effect of damping has been shown in various previous works.[9,10] The instability of an aeroelastic system can be attributed to the extraction of energy from the flow.[11] The rate of energy extraction depends on the aeroelastic mode shape (phase relationship between the pitch and plunge). Now, addition of damping can help remove some energy from the structure, but it can also change the aeroelastic mode shape. This change in the mode shape can lead to an increase in the rate of energy extraction. If the increase in the rate of energy extraction as a result of the phase change caused by the added damping is more than the rate of energy removal as a result of damping, then the damping leads to an increase in the margin of instability.

## Conclusions

The $p$ and $k$ methods predict different frequency coalescence points (flutter speeds) for the problem considered, which is to say that the $k$ method predicts an incorrect flutter speed. However, this has nothing to do with accuracy of either method. Instead, the methods provide solutions to different problems, and thus the solutions obtained from the methods have different interpretations. Because the primary interest is the flutter speed of the system, it is more relevant to consider the evolution of the system roots as a function of flight speed rather than reduced velocity. The point remains that both the methods have potential for insight into a given aeroelastic problem if the results are correctly interpreted.

## Acknowledgment

The authors thank Earl Dowell for his suggestions.

## References

[1]Fung, Y. C., *An Introduction to the Theory of Aeroelasticity*, Wiley, New York, 1955, Chap. 6.

[2]Bisplinghoff, R. L., and Ashley, H., *Principles of Aeroelasticity*, Wiley, New York, 1962, Chap. 6.

[3]Dowell, E. H. (ed.), *A Modern Course in Aeroelasticity*, 3rd ed., Kluwer Academic, Norwell, MA, 1995, Chap. 3.

[4]Pines, S., "An Elementary Explanation of the Flutter Mechanism," *Proceedings of the National Specialists Meeting on Dynamics and Aeroelasticity*, Inst. of the Aeronautical Sciences, Fort Worth, TX, 1958, pp. 52–58.

[5]Hassig, H. J., "An Approximate True Damping Solution of the Flutter Equation by Determinant Iteration," *Journal of Aircraft*, Vol. 8, No. 11, 1971, pp. 885–889.

[6]Rodden, W. P., and Bellinger, E. D., "Aerodynamic Lag Functions, Divergence, and the British Flutter Method," *Journal of Aircraft*, Vol. 19, No. 7, 1982, pp. 596–598.

[7]Hodges, D. H., and Pierce, G. A., *Introduction to Structural Dynamics and Aeroelasticity*, Cambridge Univ. Press, Cambridge, England, U.K., 2002, Chap. 4.

[8]Bisplinghoff, R. L., Ashley, H., and Halfman, R. L., *Aeroelasticity*, Addison Wesley Longman, Reading, MA, 1955, Chap. 9.

[9]Herrmann, G., and Jong, I.-C., "On the Destabilizing Effect of Damping in Nonconservative Elastic Systems," *Journal of Applied Mechanics*, Vol. 32, No. 3, 1965, pp. 592–597.

[10]Nissim, E., "Effect of Linear Damping on Flutter Speed. Part I: Binary Systems," *The Aeronautical Quarterly*, Vol. 16, May 1965, pp. 159–178.

[11]Patil, M. J., "From Fluttering Wings to Flapping Flight: The Energy Connection," *Journal of Aircraft*, Vol. 40, No. 2, 2003, pp. 270–276.

# Effects of Active and Passive Flow Control on Dynamic-Stall Vortex Formation

Lance W. Traub,* Adam Miller,† and Othon Rediniotis‡
*Texas A&M University, College Station, Texas 77843-3141*

## Introduction

EFFECTS of dynamic stall are regarded as aerodynamically and structurally deleterious. Dynamic stall has been observed on the retreating blades of helicopters, wind turbines, and on rapidly pitching aircraft. Indicators of this stall mechanism are an extension of the linear portion of the lift curve followed by a significant and nonlinear lift overshoot. The vortical structure associated with these effects also induces large pitching-moment fluctuations associated with its advection over the wing surface. Generally, the largest lift overshoot is associated with the dynamic-stall vortex (DSV) located at the midchord position, whereas the largest moment excursion occurs with DSV passage over the wing trailing edge.[1] Experimental evidence suggests that the convection velocity of the DSV is to first-order constant (at approximately $\frac{1}{3}$ of the freestream) and is independent of pitch rate or airfoil shape.[1] Four mechanisms have been suggested as causative in DSV formation[2]: 1) bursting of the leading-edge laminar separation bubble, 2) transonic flow near the leading edge, 3) separation of the turbulent flow following closure of the laminar separation bubble, and 4) reverse flow near the leading edge stemming from the upstream penetrating reverse layer associated with trailing edge stall.

Received 21 May 2003; revision received 30 May 2003; accepted for publication 2 June 2003. 

*TEES Research Scientist/Lecturer, Aerospace Engineering Department.
†Graduate Student, Aerospace Engineering Department. Student Member AIAA.
‡Associate Professor, Aerospace Engineering Department. Associate Fellow AIAA.

Studies have indicated that the chordwise location of DSV formation differs from airfoil to finite wing.[3] Concern with the effects of the DSV has promulgated studies aimed at suppressing its formation. Active flow-control methodologies such as pulsed vortex generators or slot suction have shown the ability to delay the onset of DSV formation.[4,5]

Recent advances in flow-control technology have provided means whereby fluid flow can be controlled or even restructured for relatively low energy and complexity expenditure. These advances are epitomized by the synthetic jet actuator (SJA), which has been the subject of widespread study.[6–9] All SJA actuators basically consist of a cavity, which is bounded by a moving wall on one side, and an inlet/exit slot on another. Oscillation of the wall (or piston—depending on the particular method of implementing the jet) causes a periodic inflow and outflow of fluid, such that no net mass is transferred. A momentum balance over the exit slot indicates that momentum transfer is finite, as the inflow area greatly exceeds that of outflow. The jet can be exhausted in a "Coanda" fashion, parallel to the surface, or can be inclined relative to the surface. The mechanism for synthetic jet operation is well documented.[10] Shear layers are, in general, highly receptive to disturbances. The SJA, when pulsed in the correct frequency range, can cause the shear layer to resonate, which is associated with the formation of coherent structures. The shear layer generally locks into the driving frequency or one of its harmonics. As a result, the shear layer forms discrete vortices. As they advect downstream, these vortices behave in a similar fashion to those injected by conventional vortex generators. They mix high-momentum freestream fluid into the boundary layer, energizing it.

In this Note, an experimental investigation into the effects of a SJA working in concert with fixed vortex generators (VG) on a ramping NACA 0015 wing is explored. Conventional VGs have found widespread use and application, and their interaction with potentially retrofitted active flow-control mechanisms is of interest. Presented data encompass integrated pressures yielding forces and moments for two ramp rates.

## Experimental Equipment and Procedure

The SJA employed in this investigation has been widely detailed and for conciseness will be described briefly. The SJA driving mechanism consists of a dc motor with its shaft connected eccentrically to a crank, which is in turn connected to the piston of the SJA. Due to the eccentricity, the rotary motion of the motor is translated to linear motion of the SJA membrane/piston. The motors drive a series of "off-the-shelf" small gasoline engines, which are used as reciprocating compressors. The cylinder head of each of these engines is open and attached to a plenum, which is closed on all sides except for a slot machined on one of the walls. The change in the cavity volume of the plenum causes the pressure inside the cavity to fluctuate, creating the synthetic jet. The SJA array is composed of six reciprocating compressors (pistons), which are driven by two dc motors. The exit slot of the plenum is curved in order to permit the jet to exit tangentially to the surface of the wing, taking advantage of the Coanda effect. The reader is referred to Refs. 6 and 7 for a more comprehensive description. The wind-tunnel model, presented in Fig. 1a, was machined in two halves using a computer numerically controlled (CNC) mill. The wing's profile was that of a NACA 0015. The upper wing half was made from Plexiglas®. The lower surface was machined from aluminum. The wing chord was 420 mm. Tests were undertaken at a freestream velocity of 20 m/s giving a chord-based Reynolds number of $0.57 \times 10^6$. Boundary-layer transition was enforced using trip strips located at approximately 5% of the chord on the upper and lower surfaces. No wind-tunnel wall interference or blockage corrections were applied to the data, as their application for dynamic motions is uncertain at best. The wing contained the synthetic jet actuator described earlier. The SJA exit slot was located at 12% of the chord and ejected the jet tangentially to the surface. This location was dictated by geometric considerations. The vortex generators were delta shaped with a sweep angle of 70 deg. When present, they were located at either 9% of the chord (VG1) or 16.6% of the chord (VG2) (see Fig. 1a).

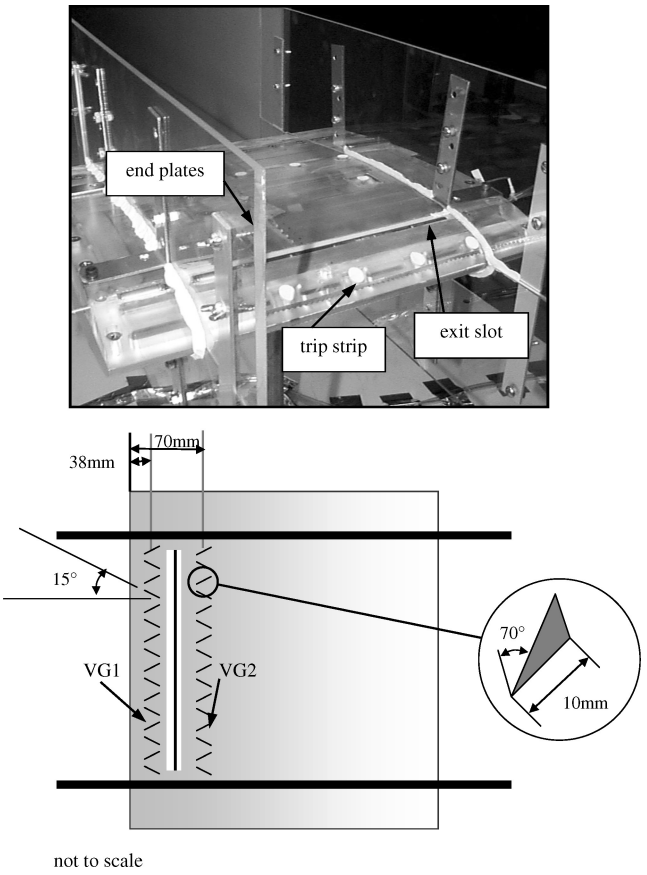


**Fig. 1a Model geometric details.**

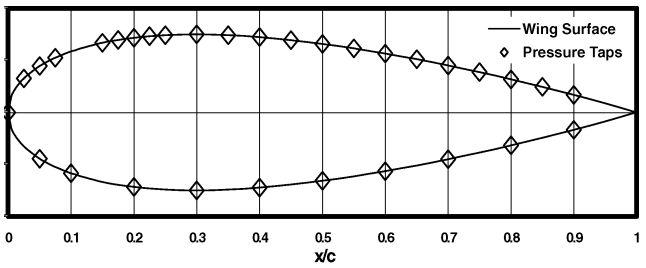


**Fig. 1b Pressure port locations.**

Surface pressures were measured over the wing using a 32-channel electronic scanning pressure (ESP) pressure scanner. The range of the 32 embedded transducers was $\pm 10$ in $H_2O$ ($\pm 2.49$ kPa). Location of the ports is given in Fig. 1b and Table 1. The method of Wildhack[11] was used to correct for acoustic effects in the employed tubing. To ensure quasi-two-dimensional behavior, side plates were mounted on the wing. Subsequent data presentation will suggest that the small size of the end plates did not allow the achievement of two-dimensional flow. However, mechanical pitching considerations eliminated the use of large plates. Forces and moments were calculated through integration of the pressure distribution around the wing. The upper and lower surface-pressure traces were fitted using cubic splines. The splines were then integrated to yield forces and moments. Presented moment coefficients are about the quarter-chord. The wing pitching motion was controlled using a stepper motor (SLO-SYN) controlled by a microlynx™ stepper motor controller. The stepper motor was connected directly to the wing's pitch strut. During a pitch test, wing position was recorded using an encoder mounted on the stepper shaft. Data from the ESP were digitized using a 16-bit computer boards A/D board. Each presented data set is comprised of 30 ensemble averages runs.

**Table 1 Pressure port locations**

| $x/c$,[a] upper | $y/c$,[b] upper | $x/c$, lower | $y/c$, lower |
|---|---|---|---|
| 0 | 0 | 0.05 | 0.044 |
| 0.025 | 0.032 | 0.1 | 0.058 |
| 0.05 | 0.044 | 0.2 | 0.071 |
| 0.075 | 0.052 | 0.3 | 0.074 |
| 0.15 | 0.066 | 0.4 | 0.072 |
| 0.175 | 0.069 | 0.5 | 0.065 |
| 0.2 | 0.071 | 0.6 | 0.056 |
| 0.225 | 0.073 | 0.7 | 0.045 |
| 0.25 | 0.074 | 0.8 | 0.031 |
| 0.3 | 0.074 | 0.9 | 0.016 |
| 0.35 | 0.074 | —— | —— |
| 0.4 | 0.072 | —— | —— |
| 0.45 | 0.069 | —— | —— |
| 0.5 | 0.065 | —— | —— |
| 0.55 | 0.061 | —— | —— |
| 0.6 | 0.056 | —— | —— |
| 0.65 | 0.050 | —— | —— |
| 0.7 | 0.045 | —— | —— |
| 0.75 | 0.038 | —— | —— |
| 0.8 | 0.031 | —— | —— |
| 0.85 | 0.024 | —— | —— |
| 0.9 | 0.016 | —— | —— |

[a]$x/c$-axial coordinate. [b]$y/c$-vertical coordinate.

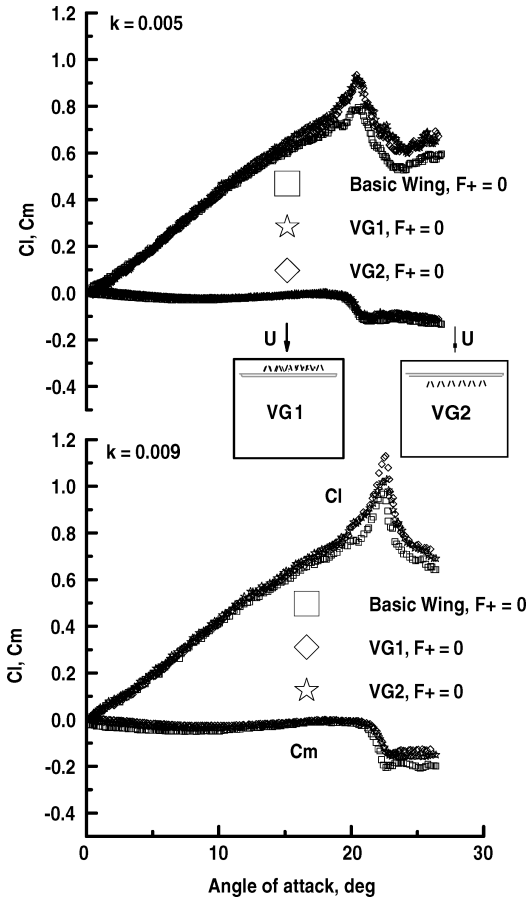


**Fig. 2 Effect of vortex generator presence and location on calculated lift and quarter-chord pitching moment.**

## Results and Discussion

In all experiments, the wing was ramped at a constant angular velocity from 0 to 27 deg. Data are presented detailing the effects of the SJA and VGs on lift coefficient (Cl) and quarter-chord pitching moment (Cm). The SJA exit slot width was 1.2 mm. $F+=1$ corresponds to a jet momentum coefficient ($C\mu$, $C\mu = 2V_{\text{rms}}^2 sw/U^2 c$) of 0.009, where $V_{\text{rms}}$ is the rms of the jet exit velocity, $sw$ is the slot width (= 1.2 mm), $U$ is the freestream (= 20 m/s), and $c$ is the chord (= 420 mm). $F+$ is the nondimensional SJA actuation frequency and is given by $F+ = fx/U$, where $f$ is the actuator frequency and $x$ is the distance from the SJA to the trailing edge. Prior studies[12] have suggested that depending on the SJA configuration and requirement a value of $F+ \approx 1$ is optimal as it corresponds to the presence of approximately 2–4 convecting vortical structures over the upper surface. The basic wing moniker refers to no actuation and VG presence.

Figure 2 presents the effect of the VGs at locations VG1 and VG2 for the two ramp rates. A nondimensional pitch rate $k$ ($k = \omega c/U$, where $\omega$ is the average angular pitch velocity) of 0.005 corresponds to a motion of 27 deg in 2 s and $k = 0.009$ corresponds to 27 deg in 1 s. For this data set, no fluidic actuation was present. At the lower pitch rate $k = 0.005$, the effect of VG presence is to augment the strength of the DSV formation (higher Cl), while causing it to occur slightly earlier then the basic wing case. The rounding of the lift curve before stall, associated with the onset and upstream progression of trailing edge stall, is lessened, presumably due to boundary-layer momentum addition caused by the streamwise vorticity injected by the VGs. The effect of the location of the two VGs, within the experimental resolution, appears marginal. For $k = 0.009$, an effect of VG location is apparent. The more aft VG location (VG2) experiences a lower loading peak then VG1. Note that the rest of the lift and moment behavior is similar. Both data sets with vortex generators show a wider DSV lift footprint then the basic wing, suggesting a lower convection velocity over the upper surface. The rate of lift increase (local slope) is greater for the basic wing, perhaps because of the VG-injected axial vorticity slowing the rate of flow separation. It is thus possible that the DSV increases in strength more rapidly for the basic wing, and consequently it can be severed from its vorticity source sooner.

Effects of fluidic actuation in concert with VG1 are presented in Fig. 3 for $k = 0.005$ and 0.009. For both pitch rates, the effect of the SJA is marked, with both a delay in the onset of the DSV (extends the

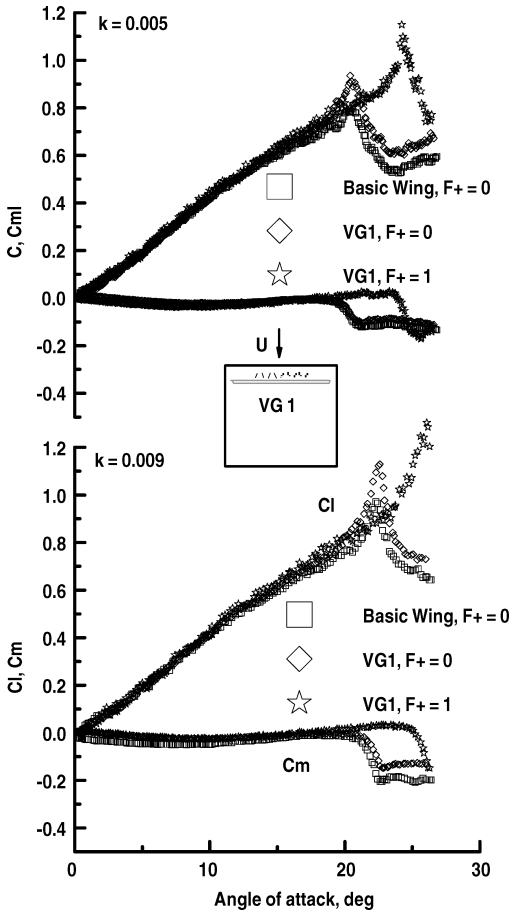


**Fig. 3 Effect of fluidic actuation on vortex generator location VG1.**

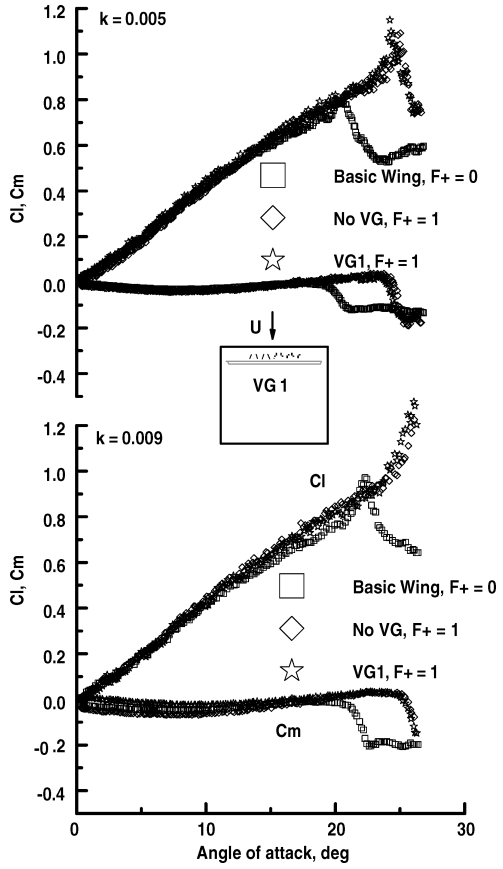


**Fig. 4 Effect of fluidic actuation with and without vortex generators present VG1.**

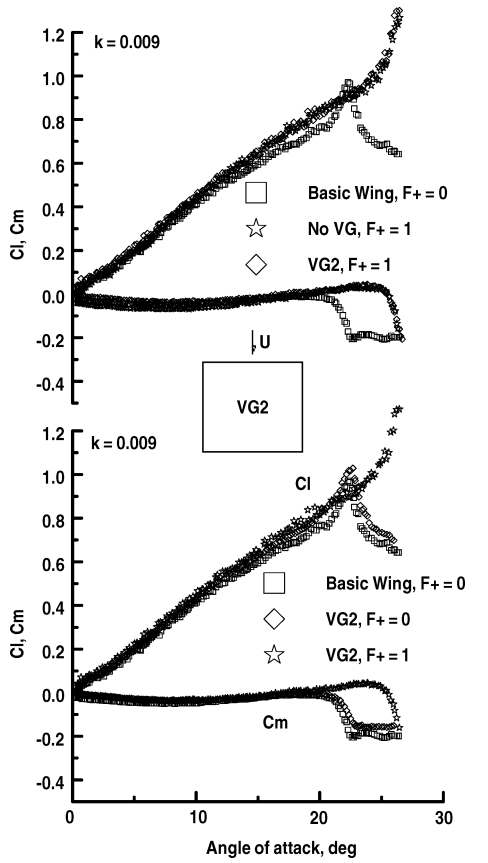


**Fig. 5 Effects of fluidic actuation and presence of vortex generator VG2.**

linear portion of the lift curve) and a significant increase in the level of lift augmentation. Explicit effects of the first vortex generator configuration VG1 in concert with the SJA, $F+=1$, are shown in Fig. 4 for $k=0.005$ and 0.009. The presence of the VGs is seen to have a small effect on the calculated loads and moments. With the vortex generator present, the onset of the DSV occurs at a slightly lower incidence, and the peak vortex-induced suction is seen to be somewhat larger. This could be due to augmented vortex strength or closer vortex-wing proximity. Effects of the second VG location VG2, both with and without the SJA, are presented in Fig. 5. As observed for VG1, the vortex generators augment the DSV-induced loading, but in concert with the SJA loading is greatly increased while nonlinear effects are delayed to higher incidence. With $F+=1$, VG2 is seen to have no effect within the experimental resolution whereas a small effect was noted for VG1.

## Conclusions

A low-speed wind-tunnel investigation has been undertaken to determine the effect of synthetic jet actuation in combination with fixed vortex generators on an airfoil performing a linear ramping motion. An instrumented NACA 0015 wing was ramped from 0–27 deg at two pitch rates during which surface pressures were recorded. The pressures were integrated to yield forces and moments. The data indicate that in the absence of fluidic actuation the tested vortex generator configurations do not delay the onset of the dynamic-stall vortex, but they do augment its induced loading and delay viscous effects. In concert with the synthetic jet, the effect of the vortex generators was marginal, although a moderate dependency on vortex generator location was evident.

## Acknowledgments

This work was sponsored by the U.S. Air Force Office of Scientific Research, (AFOSR), under the Contract F49620-01-1-0012 and by U.S. Air Force Research Laboratory through the Small Business Initiative Research (SBIR) Program (in collaboration with Aeroprobe Corporation). The authors would like to thank T. Beutner, the monitor for the AFOSR project, and J. Myatt and C. Camphouse, the monitors of the SBIR project.

## References

[1]Green, R. B., Galbraith, R. A., and Niven, A. J., "Measurements of the Dynamic Stall Vortex Convection Speed," *The Aeronautical Journal*, Vol. 96, Oct. 1992, pp. 319–325.

[2]McCroskey, W. J., Carr, L. W., and Mcalister, K. W., "Dynamic Stall Experiments on Oscillating Aerofoils," *AIAA Journal*, Vol. 14, No. 4, 1976, pp. 57–63.

[3]Ferrecchia, A., Coton, F. N., and Gailbraith, R. A., "An Examination of Dynamic Stall Vortex Inception on a Finite Wing and on a NACA 0015 Aerofoil," AIAA June–July 1999.

[4]Magill, J. C., and McManus, K. R., "Control of Dynamic Stall using Pulsed Vortex Generator Jets," AIAA Paper 98-0675, 1998.

[5]Alrefai, M., and Acharya, M., "Controlling Leading-Edge Suction for the Management of Unsteady Separation over Pitching Airfoils," AIAA Paper 95-2188, June 1995.

[6]Gilarranz, J. L., Traub, L. W., and Rediniotis, O. K., "Characterization of a Compact, High-Power Synthetic Jet Actuator for Flow Separation Control," AIAA Paper 2002-0127, Jan. 2002.

[7]Gilarranz, J. L., and Rediniotis, O. K., "Compact, High-Power Synthetic Jet Actuators for Flow Separation Control," AIAA Paper 2001-0737, Jan. 2001.

[8]Amitay, M., and Glezer, A., "Role of Actuation Frequency in Controlled Flow Reattachment over a Stalled Airfoil," *AIAA Journal*, Vol. 40, No. 2, 2002, pp. 209–216.

[9]Traub, L. W., Miller, A., and Rediniotis, O., "Effects of Synthetic Jet Actuation on a Pitching NACA 0015," *Journal of Aircraft* (accepted for publication).

[10]Wu, J. Z., Lu, X., Denny, A. G., Fan, M., and Wu, J., "Post-Stall Flow Control on an Airfoil by Local Unsteady Forcing," *Journal of Fluid Mechanics*, Vol. 371, 1998, pp. 21–58.

[11]Wildhack, W. A., "Pressure Drop in Tubing in Aircraft Instrument Installations," NACA TN-593 , Feb. 1937, p. 30.

[12]Seifert, A., Eliahu, S., Greenblatt, D., and Wygnanski, I., "On the Use of Piezoelectric Actuators for Airfoil Separation Control," *AIAA Journal*, Vol. 36, No. 8, 1998, pp. 1535–1537.